Radiolabeled somatostatin receptor antagonists are preferable to agonists for *in vivo* peptide receptor targeting of tumors

Mihaela Ginj*, Hanwen Zhang*, Beatrice Waser†, Renzo Cescato†, Damian Wild*, Xuejuan Wang*, Judit Erchegyi‡, Jean Rivier‡, Helmut R. Mäcke*, and Jean Claude Reubi†§

*Division of Radiological Chemistry, Institute of Nuclear Medicine, Department of Radiology, University Hospital Basel, Petersgraben 4, CH-4031 Basel, Switzerland; †Division of Cell Biology and Experimental Cancer Research, Institute of Pathology, University of Berne, Murtenstrasse 31, CH-3010 Berne, Switzerland; and ‡Clayton Foundation Laboratories for Peptide Biology, The Salk Institute, 10010 North Torrey Pines Road, La Jolla, CA 92037

Communicated by Roger Guillemin, The Salk Institute for Biological Studies, La Jolla, CA, September 5, 2006 (received for review May 6, 2006)

Targeting neuroendocrine tumors expressing somatostatin receptor subtypes (sst) with radiolabeled somatostatin agonists is an established diagnostic and therapeutic approach in oncology. While agonists readily internalize into tumor cells, permitting accumulation of radioactivity, radiolabeled antagonists do not, and they have not been considered for tumor targeting. The macrocyclic chelator 1,4,7,10-tetraazacyclododecane-1,4,7,10-tetraacetic acid (DOTA) was coupled to two potent somatostatin receptor-selective peptide antagonists [NH_2-CO-c(DCys-Phe-Tyr-DAgl^8(Me,2-naphthoyl)-Lys-Thr-Phe-Cys)-OH (sst_3-ODN-8) and a sst_2-selective antagonist (sst_2-ANT)], for labeling with $^{111/nat}$In. $^{111/nat}$In-DOTA-sst_3-ODN-8 and $^{111/nat}$In-DOTA–[4-NO_2-Phe-c(DCys-Tyr-DTrp-Lys-Thr-Cys)-DTyr-NH_2] ($^{111/nat}$In-DOTA-sst_2-ANT) showed high sst_3- and sst_2-binding affinity, respectively. They did not trigger sst_3 or sst_2 internalization but prevented agonist-stimulated internalization. ^{111}In-DOTA-sst_3-ODN-8 and ^{111}In-DOTA-sst_2-ANT were injected intravenously into mice bearing sst_3- and sst_2-expressing tumors, and their biodistribution was monitored. In the sst_3-expressing tumors, strong accumulation of ^{111}In-DOTA-sst_3-ODN-8 was observed, peaking at 1 h with 60% injected radioactivity per gram of tissue and remaining at a high level for >72 h. Excess of sst_3-ODN-8 blocked uptake. As a control, the potent agonist ^{111}In-DOTA–[1-Nal^3]-octreotide, with strong sst_3-binding and internalization properties showed a much lower and shorter-lasting uptake in sst_3-expressing tumors. Similarly, ^{111}In-DOTA-sst_2-ANT was injected into mice bearing sst_2-expressing tumors. Tumor uptake was considerably higher than with the highly potent sst_2-selective agonist ^{111}In-diethylenetriaminepentaacetic acid–[Tyr^3,Thr^8]-octreotide (^{111}In-DTPA-TATE). Scatchard plots showed that antagonists labeled many more sites than agonists. Somatostatin antagonist radiotracers therefore are preferable over agonists for the *in vivo* targeting of sst_3- or sst_2-expressing tumors. Antagonist radioligands for other peptide receptors need to be evaluated in nuclear oncology as a result of this paradigm shift.

antagonist radioligands | tumor targeting | peptide hormones | neuropeptides | receptor internalization

Peptide receptor targeting *in vivo* is a successful method to image and treat various types of cancers (1). The best example is somatostatin receptor targeting with ^{111}In-, ^{90}Y-, or ^{177}Lu-labeled somatostatin radioligands that are injected into the patients intravenously and accumulate in their somatostatin receptor-expressing tumors. For this purpose, agonists have been selected. The rationale is that agonists, after high-affinity binding to the receptor, usually trigger internalization of the ligand–receptor complex (2). This process of internalization is the basis for an efficient accumulation of the radioligand in a cell over time (1, 3–5), and it has been considered a crucial step in the process of *in vivo* receptor targeting with radiolabeled peptides (4–6). Recently, a highly significant correlation between the rate of ligand internalization *in vitro* into AR42J cells expressing somatostatin receptor subtype 2 (sst_2) and the *in vivo* uptake in the sst_2-expressing rat tumor model has been reported (7). Therefore, when novel analogs are being designed for receptor targeting, their internalization properties are particularly thoroughly investigated (3).

Curiously, not much is known about the usefulness, for *in vivo* targeting of cancer, of high binding-affinity compounds lacking the ability to trigger receptor internalization. In this respect, little is known about antagonists, which, with a few exceptions (8–11), do not internalize (8, 12, 13), and one could therefore expect them not to be of particular interest as radioligands for receptor targeting. However, antagonists may have characteristics other than those related to internalization that may make their radiolabeled derivatives suitable tools for *in vivo* receptor targeting. Most relevant is the *in vitro* evidence that, in certain circumstances, antagonist radioligands may label a higher number of receptor-binding sites than agonist radioligands (14, 15).

The aim of the present study was to investigate to which extent somatostatin antagonist and agonist radioligands, with similar binding affinities for somatostatin receptors, differ in their *in vivo* tumor-targeting properties. The best clinically established system for *in vivo* tumor targeting with radiolabeled peptides (1) is based on the somatostatin receptor, and a particularly large number of excellent radioligands have been developed for that purpose, all derived from somatostatin agonists (16). The first part of the present study deals with somatostatin receptor subtype 3 (sst_3). First, sst_3 is characterized by very efficient internalization properties (17). Second, recently, sst_3-selective antagonists with high binding affinity but without triggering receptor internalization have been described (18). Their radiolabeled derivatives may be used as antagonist radioligands in case the high affinity-binding and antagonistic properties are retained after conjugation with a chelator [e.g., 1,4,7,10-tetraazacyclododecane-1,4,7,10-tetraacetic acid (DOTA)] and ^{111}In-complexation. Third, well characterized radiolabeled agonists, which can label sst_3 receptors *in vitro* and *in vivo*, have recently been described (19–21) and can be used as reference

Author contributions: M.G. and H.Z. contributed equally to this work; H.R.M., and J.C.R. designed research; M.G., H.Z., B.W., R.C., D.W., and X.W. performed research; J.E., J.R., and H.R.M. contributed new reagents/analytic tools; M.G., H.Z., R.C., J.R., H.R.M., and J.C.R. analyzed data; and J.C.R. wrote the paper.

The authors declare no conflict of interest.

Freely available online through the PNAS open access option.

Abbreviations: sst, somatostatin receptor subtype; DOTA, 1,4,7,10-tetraazacyclododecane-1,4,7,10-tetraacetic acid; NOC, [1-Nal^3]-octreotide; DTPA, diethylenetriaminepentaacetic acid; TATE, [Tyr^3,Thr^8]-octreotide; sst_3-ODN-8, NH_2-CO-c(DCys-Phe-Tyr-DAgl^8(Me,2-naphthoyl)-Lys-Thr-Phe-Cys)-OH; sst_2-ANT, [Ac-4-NO_2-Phe-c(DCys-Tyr-DTrp-Lys-Thr-Cys)-DTyr-NH_2]; IA/g, injected activity per gram of tissue; CCL-sst_3, CCL39 cells stably expressing sst_3; HEK-sst_3, HEK293 cells stably expressing sst_3; SS-28, somatostatin-28.

§To whom correspondence should be addressed. E-mail: reubi@pathology.unibe.ch.

Table 1. *In vitro* binding, signaling, and internalization properties of somatostatin analogs

	Binding affinity*						
	sst_1	sst_2	sst_3	sst_4	sst_5	Signaling†	Internalization
Antagonists							
sst_3-ODN-8	>1,000	>1,000	8.6 ± 1.87	>1,000	>1,000	Antagonist (sst_3)	No internalization (sst_3)
DOTA-sst_3-ODN-8	>1,000	>1,000	5.2 ± 1.3	>1,000	>1,000	Antagonist (sst_3)	No internalization (sst_3)
^{nat}In-DOTA-sst_3-ODN-8	>1,000	>1,000	15 ± 5.2	>1,000	>1,000	Antagonist (sst_3)	No internalization (sst_3)
sst_2-ANT	>1,000	3.6 ± 0.4	>1,000	349 ± 30	276 ± 119	Antagonist (sst_2)	No internalization (sst_2)
DOTA-sst_2-ANT	>1,000	1.5 ± 0.4	>1,000	287 ± 27	>1,000	Antagonist (sst_2)	No internalization (sst_2)
^{nat}In-DOTA-sst_2-ANT	>1,000	9.4 ± 0.4	>1,000	380 ± 57	>1,000	Antagonist (sst_2)	No internalization (sst_2)
Agonists							
SS-28	3.2 ± 0.2	2.3 ± 0.1	3.7 ± 0.3	2.6 ± 0.1	2.4 ± 0.2	Agonist (all sst)	Internalization ($sst_{2,3,5}$)
^{nat}In-DOTA-NOC	>1,000	2.9 ± 0.3	11 ± 3.2	503 ± 222	9.4 ± 3.7	Agonist ($sst_{2,3}$)	Internalization ($sst_{2,3}$)
^{nat}In-DTPA-TATE	>1,000	1.3 ± 0.2	>1,000	>1,000	>1,000	Agonist (sst_2)‡	Internalization (sst_2)‡

*Values represent IC_{50} in nM; mean ± SEM $n \geq 3$.
†Tested with cAMP assay in sst-transfected cells.
‡Tested as DTPA-TATE.

compounds in parallel experiments. Therefore, we have coupled the chelator DOTA to the sst_3 antagonist NH_2-CO-c(DCys-Phe-Tyr-DAgl^8(Me,2-naphthoyl)-Lys-Thr-Phe-Cys)-OH (sst_3-ODN-8), labeled the conjugate with nonradioactive ^{nat}In, and tested ^{nat}In-DOTA-sst_3-ODN-8 for *in vitro* binding and signaling properties to establish whether it is suitable to be used for *in vivo* receptor targeting. We then compared the *in vivo* biodistribution of the ^{111}In-labeled antagonist ^{111}In-DOTA-sst_3-ODN-8 with that of a similarly potent and well established agonist-radioligand ^{111}In-DOTA-[1-Nal^3]-octreotide (^{111}In-DOTA-NOC) in an sst_3 tumor-bearing nude mouse model. The properties of each compound to target normal and neoplastic tissue *in vivo* have been assessed quantitatively.

In a second part, we have performed comparable studies with the sst_2 receptor system, to generalize the sst_3-related observations. By using the same strategy, we have developed an ^{nat}In- or ^{111}In-labeled sst_2 antagonist $^{111/nat}$In-DOTA-[4-NO_2-Phe-c(DCys-Tyr-DTrp-Lys-Thr-Cys)-DTyr-NH_2] ($^{111/nat}$In-DOTA-sst_2-ANT), characterized it in *in vitro* experiments, and compared its *in vivo* sst_2 tumor-targeting properties to that of the highly potent sst_2 agonist ^{111}In- diethylenetriaminepentaacetic acid –[Tyr^3,Thr^8]-octreotide (^{111}In-DTPA-TATE) (ref. 22) in mice.

Results

Table 1 summarizes the binding data of the sst_3 antagonist (sst_3-ODN-8) and its DOTA analog with or without ^{nat}In complexation at all five sst. For comparison, the values of the natural somatostatin-28 (SS-28) as well as that of a potent sst_3 agonist, ^{nat}In-DOTA-NOC, are shown as references. sst_3-ODN-8 and its derivatives show high selectivity and binding affinity for sst_3. The reference agonist ^{nat}In-DOTA-NOC has comparable sst_3-binding affinity, whereas the sst_2-selective analog (^{nat}In-DTPA-TATE), used in its ^{111}In-labeled form as a negative control for sst_3-expressing tissues in the biodistribution assays, shows high sst_2 but no sst_3 affinity (Table 1).

The compounds were evaluated for their effect on forskolin-stimulated cAMP accumulation in CCL39 cells stably expressing sst_3 (Table 1). SS-28 and ^{nat}In-DOTA-NOC, used as controls, act as agonists; they potently inhibit forskolin-stimulated cAMP accumulation by >77% and 58%, respectively, at a peptide concentration of 100 nM. sst_3-ODN-8 and its two derivatives given alone do not inhibit forskolin-stimulated cAMP accumulation up to 10 μM. However, the agonistic effect of SS-28 can be competitively antagonized with a fixed concentration of 1 μM each of the sst_3-ODN-8 derivatives applied individually. Fig. 1*B* illustrates the antagonistic properties of the sst_3-ODN-8 derivatives.

The antagonistic property of DOTA-sst_3-ODN-8 and its derivatives was also confirmed in an immunofluorescence internalization assay (3) with HEK293 cells stably expressing sst_3 (Table 1). Fig. 1*C* illustrates that, although the control agonists SS-28 and ^{nat}In-DOTA-NOC can induce sst_3 internalization, the DOTA-sst_3-ODN-8 analogs have no effect when given alone, even at a concentration of 10 μM. Moreover, they prevent sst_3 internalization induced by SS-28 (Fig. 1*C*) or by the agonist ^{nat}In-DOTA-NOC.

Furthermore, Fig. 1*D* shows a Scatchard analysis in HEK-sst_3 cells comparing the B_{max} for the agonist ^{111}In-DOTA-NOC (68 ± 9 pM) with that of the antagonist ^{111}In-DOTA-sst_3-ODN-8 (5,180 ± 70 pM). The antagonist labels 76 times more sst_3 sites in cultured HEK-sst_3 cells than the agonist.

In Tables 2 and 3, the *in vivo* biodistribution of the antagonist ^{111}In-DOTA-sst_3-ODN-8 is reported in nude mice bearing the sst_3-expressing tumor (Table 2) and compared with that of the agonist ^{111}In-DOTA-NOC (Table 3). Of note is the accumulation of the radiolabeled antagonist in the tumor, which peaks at 1 h [>60% injected activity per gram of tissue (IA/g) uptake] and remains very high at 4 h (50%IA/g), at 24 h (>30%IA/g) and even at 72 h (>10%IA/g). The pituitary, an organ known to express various sst, including sst_3 (17), is also labeled with the antagonist ^{111}In-DOTA-sst_3-ODN-8 (Table 2). A blocking experiment performed in separate mice by adding 1,000 times excess of sst_3-ODN-8 together with the radioligand documents that the majority of the labeling in the sst_3-expressing tumor and pituitary represents binding to specific somatostatin receptors. The blocking agent did not affect radioactivity uptake in the kidneys and blood, indicating that this uptake is not receptor-mediated (Table 2). For comparison, the accumulation of radioactivity in the sst_3-expressing tumors by using the agonist ^{111}In-DOTA-NOC is considerably less than by using the antagonist ^{111}In-DOTA-sst_3-ODN-8 and amounts to ≈7%IA/g at 4 h and decreases at 24 h (Table 3). The calculated tumor/tissue ratios, representing important parameters to evaluate the quality of a targeting agent (16), are considerably higher with ^{111}In-DOTA-sst_3-ODN-8 than with ^{111}In-DOTA-NOC, especially for the tumor/blood and tumor/muscle ratios at 4 and 24 h. Established sst_2-expressing organs, such as the stomach, adrenals, or pancreas, show a blockable accumulation of ^{111}In-DOTA-NOC (Table 3), whereas they show no significant accumulation of ^{111}In-DOTA-sst_3-ODN-8 (Table 2). As a negative control, labeling of the sst_3-expressing tumor with a specific sst_2

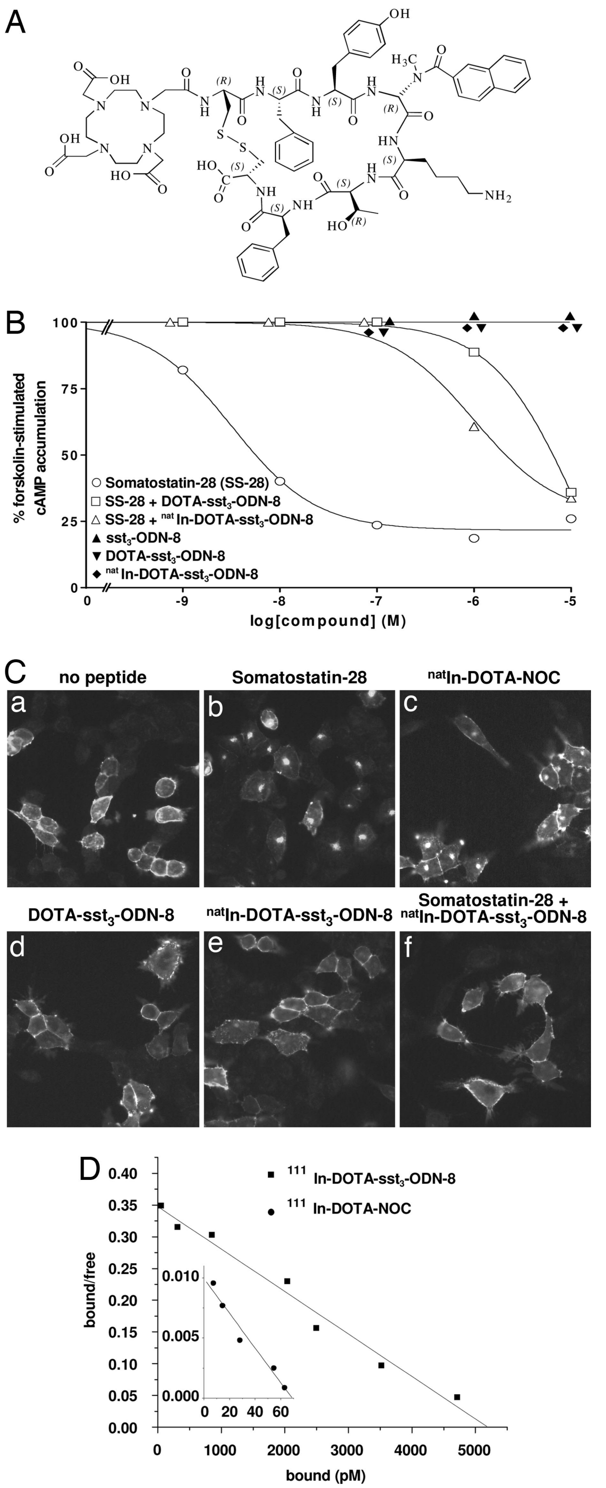

Fig. 1. *In vitro* characteristics of somatostatin analogs. (*A*) Structure of the sst_3 antagonist DOTA-sst_3-ODN-8. (*B*) Effects of somatostatin analogs on forskolin-stimulated cAMP accumulation in CCL-sst_3 cells. Concentration-response curves with increasing concentrations of SS-28 (○), sst_3-ODN-8 (▲), DOTA-sst_3-ODN-8 (▼), or ^{nat}In-DOTA-sst_3-ODN-8 (◆), and of increasing concentrations of SS-28 in the presence of 10^{-6} M DOTA-sst_3-ODN-8 (□) or 10^{-6} M ^{nat}In-DOTA-sst_3-ODN-8 (△). Data are expressed as a percentage of the 10 μM forskolin response. SS-28 inhibits forskolin-stimulated cAMP formation in CCL-sst_3 cells, whereas the sst_3-ODN-8 derivatives alone have no effect; however, they reverse the SS-28-induced effect on cAMP. (*C*) Effect of soma tostatin analogs on sst_3 internalization detected by immunofluorescence in HEK-sst_3 cells. Control experiment showing membrane-bound sst_3 with no peptide (*a*); 100 nM of the agonists SS-28 (*b*), or ^{nat}In-DOTA-NOC (*c*) trigger sst_3 internalization. The antagonist DOTA-sst_3-ODN-8 (*d*) or its ^{nat}In-derivative (*e*) at 10 μM are not able to induce internalization. Internalization triggered by 100 nM of SS-28 is abolished by 10 μM ^{nat}In-DOTA-sst_3-ODN-8 (*f*). (*D*) Scatchard plots from saturation-binding experiments on HEK-sst_3 cells show a higher B_{max} for ^{111}In-DOTA-sst_3-ODN-8 than for ^{111}In-DOTA-NOC.

agonist radioligand, ^{111}In-DTPA-TATE (22), is found to be negligible (Table 3). The high uptake of ^{111}In-DOTA-NOC and ^{111}In-DTPA-TATE in the pituitary reflects the high expression of sst_2 in this organ. Fig. 2 shows scans taken at 30 min and 4 h of animals bearing sst_3-expressing tumors in one flank and, as control, sst_2-expressing tumors in the other flank. Mice injected with the sst_3 antagonist ^{111}In-DOTA-sst_3-ODN-8 showed a massive uptake in the sst_3- but not the sst_2-expressing tumor, whereas those injected with the sst_2/sst_3 agonist ^{111}In-DOTA-NOC showed a weak uptake in both tumors.

Similarly, we investigated the sst_2 receptor system with sst_2-transfected HEK293 and CCL39 cells *in vitro* or HEK293 cells transplanted in animals, to expand the above sst_3 study. We chose to conjugate the established sst_2-ANT (23) with DOTA, namely DOTA-[4-NO_2-Phe-c(DCys-Tyr-DTrp-Lys-Thr-Cys)-DTyr-NH_2] (DOTA-sst_2-ANT). sst_2-ANT and unlabeled or In-labeled DOTA-sst_2-ANT have high binding affinity and selectivity for sst_2 (Table 1). Both the In-labeled and unlabeled DOTA-sst_2-ANT are sst_2-antagonists in the cAMP assay; although inactive at 10 μM concentration in the absence of SS-28, they reverse completely the 100 nM SS-28-induced inhibition of cAMP formation triggered by 30 μM forskolin in CCL-sst_2 cells. Further, they also act as antagonists in the immunofluorescence internalization assay, because they do not induce internalization of the sst_2 receptor up to 10,000 nM but inhibit completely at 1,000 nM the internalization induced by potent somatostatin agonists such as DTPA-TATE (Fig. 3). The tissue biodistribution after ^{111}In-DOTA-sst_2-ANT injection in mice reveals a high but also long-lasting tumor uptake in sst_2 tumor-bearing animals (Table 4). It is impressive to see that 4- and 24-h values of tumor uptake are twice the ones obtained with the highly potent sst_2 agonist ^{111}In-DTPA-TATE given under the same conditions. As proof of specificity, uptake in the tumor is massively blocked by excess DOTA-sst_2-ANT (Table 4). Moreover, Scatchard analysis in HEK-sst_2 cells identifies more sites labeled with the radiolabeled antagonist (B_{max} = 354 ± 14 pM) than with the agonist (B_{max} = 23 ± 1.0 pM).

Discussion

Agonists have been used exclusively as radioligands in the past decade for the development and implementation of peptide receptor targeting of tumors *in vivo*, because such radioligands are readily internalized together with the receptor, permitting an active accumulation of radioactivity in the tumor cells (1, 3–5). The present study may build the foundation for a change of paradigm in this respect. Indeed, it shows, unexpectedly, that adequately labeled sst_2 and sst_3 antagonists, even though they do not internalize, may be useful radioligands to target tumors *in vivo*. More importantly, it also shows that antagonists may be even better candidates to target tumors than agonists with comparable binding characteristics.

In the *in vivo* model of an sst_3-expressing tumor, we have compared the biodistribution of the sst_3 antagonist, ^{111}In-DOTA-sst_3-ODN-8, with that of an established agonist, ^{111}In-DOTA-NOC (19–21). ^{nat}In-DOTA-NOC has high binding affinity to sst_3 receptors *in vitro* (19) and efficiently triggers the sst_3 internalization into HEK-sst_3 cells. The DOTA-linked sst_3-ODN-8 antagonist, with or without indium, also shows a comparably high sst_3-binding affinity but, differently from ^{nat}In-DOTA-NOC, it cannot trigger sst_3 internalization into HEK-sst_3 cells. Therefore, although one can expect to see a specific *in vivo* uptake of ^{111}In-DOTA-NOC in

Table 2. Biodistribution in HEK-sst$_3$ tumor-bearing nude mice at 0.25, 0.5, 1, 4, 24, or 72 h after injection of ^{111}In-DOTA-sst$_3$-ODN-8

Organ	0.25 h	0.25 h, blocked*	0.5 h	1 h	4 h	24 h	72 h
Blood	10.4 ± 1.3	9.2 ± 0.5	5.3 ± 0.2	1.8 ± 0.8	0.1 ± 0.00	0.03 ± 0.01	0.01 ± 0.00
Stomach	2.7 ± 0.1	3.1 ± 0.4	2.0 ± 0.6	1.1 ± 0.6	0.2 ± 0.00	0.23 ± 0.13	0.12 ± 0.00
Kidney	20.3 ± 1.1	21.7 ± 4.9	17.8 ± 1.8	15.8 ± 3.1	14.1 ± 2.9	6.8 ± 1.2	3.5 ± 0.3
Bowel	2.4 ± 0.09	2.2 ± 0.2	1.4 ± 0.1	0.7 ± 0.3	0.17 ± 0.03	0.08 ± 0.01	0.07 ± 0.00
Pancreas	1.8 ± 0.1	1.3 ± 0.05	1.1 ± 0.1	0.5 ± 0.3	0.16 ± 0.00	0.08 ± 0.01	0.06 ± 0.00
Spleen	2.3 ± 0.08	2.4 ± 0.2	1.3 ± 0.08	0.8 ± 0.3	0.34 ± 0.04	0.17 ± 0.03	0.15 ± 0.01
Liver	3.8 ± 0.8	3.8 ± 0.04	2.1 ± 0.3	1.3 ± 0.4	0.63 ± 0.02	0.41 ± 0.21	0.18 ± 0.00
Heart	1.3 ± 0.08	1.4 ± 0.04	0.9 ± 0.05	0.6 ± 0.1	0.22 ± 0.05	0.15 ± 0.01	0.08 ± 0.00
sst$_3$ tumor	**22.1 ± 3.5**	**9.3 ± 0.2†**	**34.8 ± 1.4**	**61.3 ± 10.1**	**49.7 ± 11.8**	**30.8 ± 5.0**	**10.9 ± 1.9**
Muscle	3.6 ± 0.4	3.6 ± 0.1	2.0 ± 0.1	0.9 ± 0.6	0.2 ± 0.04	0.09 ± 0.004	0.03 ± 0.00
Adrenal	4.8 ± 0.6	3.9 ± 0.2	3.6 ± 0.2	1.7 ± 1.0	1.0 ± 0.2	0.68 ± 0.12	0.61 ± 0.08
Bone	2.1 ± 0.1	2.2 ± 0.1	1.2 ± 0.1	0.6 ± 0.2	0.2 ± 0.01	0.2 ± 0.04	0.22 ± 0.05
Pituitary	24.4 ± 0.7	7.4 ± 1.8†	14.1 ± 1.0	5.3 ± 0.6	3.6 ± 0.2	1.7 ± 0.3	1.11 ± 0.2
Tumor/tissue ratios							
Tumor/blood	2.1 ± 0.33		6.5 ± 0.26	34.0 ± 5.6	497.0 ± 98	1026 ± 166	1090 ± 190
Tumor/kidney	1.08 ± 0.1		1.95 ± 0.07	3.9 ± 0.6	3.5 ± 0.8	4.5 ± 0.7	3.1 ± 0.5
Tumor/muscle	6.1 ± 0.9		17.4 ± 0.7	68.1 ± 11	248 ± 59	342 ± 55	363 ± 63

The results are expressed as the percentage of the %IA/g, mean ± SEM, $n \geq 3$. Bold text indicates the tumor as the most important of the listed tissues.
*Blocked with excess sst$_3$-ODN-8 coinjected with the radioligand.
†$P < 0.001$.

sst$_3$-expressing tumors, it is unexpected, based on current knowledge (1, 3–5), to see such a high uptake with ^{111}In-DOTA-sst$_3$-ODN-8. The uptake in the tumors and in the sst$_3$-expressing pituitary is specific in both cases, because it can be specifically blocked by the corresponding cold peptide, indicating a somatostatin receptor-mediated process.

One of the most impressive findings is that the amount of uptake of the antagonist radioligand is particularly high in these tumors: 60%IA/g uptake has indeed never been achieved by any somatostatin receptor agonist ligand, not even by those developed most recently (19, 21). Not only is the uptake at the peak time point very high, but also the long-lasting accumulation of the antagonist radioligand up to 72 h after injection is a remarkable result and represents a considerable advantage over labeling with established agonists. Of crucial importance for potential clinical use are the high tumor/tissue ratios obtained with the radiolabeled antagonist.

The same observation of a much better labeling is obtained in HEK-sst$_2$ tumors with the sst$_2$ antagonist ^{111}In-DOTA-sst$_2$-ANT. Knowing of the outstanding targeting abilities of ^{111}In-

Table 3. Biodistribution in HEK-sst$_3$ tumor-bearing nude mice at 0.5, 4, or 24 h after injection of ^{111}In-DOTA-NOC and at 4 h after ^{111}In-DTPA-TATE

	^{111}In-DOTA-NOC				^{111}In-DTPA-TATE
Organ	0.5 h	4 h	4 h, blocked*	24 h	4 h
Blood	2.6 ± 0.3	0.3 ± 0.02	0.5 ± 0.03	0.1 ± 0.00	0.1 ± 0.01
Stomach	7.4 ± 2.0	3.4 ± 0.4	0.46 ± 0.01†	1.7 ± 0.4	5.2 ± 0.2
Kidney	11.7 ± 1.3	14.2 ± 0.8	17.9 ± 1.1	9.0 ± 1.2	17.7 ± 1.5
Bowel	1.9 ± 0.1	0.9 ± 0.1	0.3 ± 0.05	0.6 ± 0.1	1.1 ± 0.1
Pancreas	13.4 ± 3.4	2.7 ± 0.2	0.2 ± 0.02†	1.5 ± 0.1	4.8 ± 0.4
Spleen	1.7 ± 0.07	0.5 ± 0.03	2.2 ± 0.8	0.5 ± 0.09	0.5 ± 0.04
Liver	1.8 ± 0.1	0.9 ± 0.07	1.5 ± 0.7	0.6 ± 0.05	0.2 ± 0.04
Heart	1.5 ± 0.2	0.3 ± 0.03	0.3 ± 0.01	0.1 ± 0.02	0.2 ± 0.00
sst$_3$ tumor	**17.5 ± 4.3**	**6.5 ± 0.7**	**4.08 ± 0.22†**	**3.5 ± 0.2**	**0.3 ± 0.02**
Muscle	1.4 ± 0.2	0.2 ± 0.01	0.2 ± 0.01	0.1 ± 0.01	0.2 ± 0.01
Adrenal	6.5 ± 1.3	4.7 ± 0.6	0.8 ± 0.05†	2.6 ± 0.2	4.6 ± 0.2
Bone	2.6 ± 0.4	0.7 ± 0.08	0.4 ± 0.07	0.8 ± 0.1	0.7 ± 0.05
Pituitary	6.1 ± 0.5	8.3 ± 3.3	3.3 ± 0.8†	5.5 ± 0.4	18.7 ± 1.2
Tumor/tissue ratios					
Tumor/blood	6.7 ± 1.6	21.6 ± 2.3		35 ± 2	
Tumor/kidney	1.5 ± 0.3	0.45 ± 0.04		0.4 ± 0.01	
Tumor/muscle	12.5 ± 2.8	32.5 ± 3.5		35 ± 2	

The results are expressed as percentage of the %IA/g, mean ± SEM, $n \geq 3$. Bold text indicates the tumor as the most important of the listed tissues.
*Blocked with excess ^{nat}In-DOTA-NOC coinjected with the radioligand.
†$P < 0.001$.

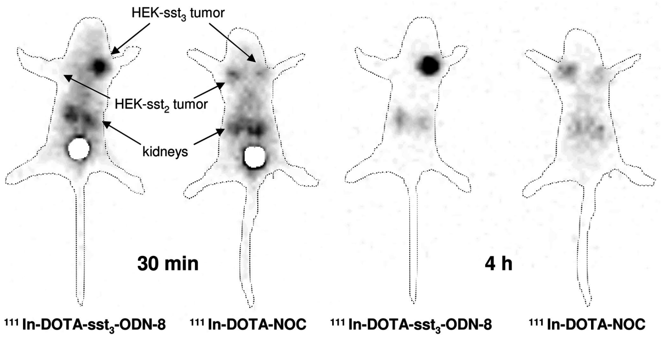

Fig. 2. *In vivo* scans taken 30 min and 4 h after injection of ^{111}In-DOTA-sst$_3$-ODN-8 or ^{111}In-DOTA-NOC. Each mouse was bearing two tumors, an sst$_3$-expressing tumor and, as control, an sst$_2$-expressing tumor. Mice were placed directly on one head of a two-headed gamma-camera system (PRISM 2000, Philips, Eindhoven, The Netherlands) equipped with medium-energy collimators (acquisition time, 10 min per time point). Strong uptake is seen with the antagonist radioligand in the sst$_3$-expressing tumor exclusively, whereas weak uptake was found in both tumors with the sst$_2$/sst$_3$ agonist.

DTPA-TATE (22), it is striking to see that the *in vivo* labeling at 4 and 24 h for the sst$_2$ antagonist is twice as high, despite the fact that the antagonist is not internalized into the tumor cells and that its sst$_2$-binding affinity is lower than for the agonist.

Explanations for these excellent *in vivo* targeting properties of antagonists may be found, at least in part, in previous *in vitro* studies dealing with other G protein-coupled receptors. Indeed, a higher number of 5-HT$_{2A}$ (15) or corticotropin releasing factor (CRF) receptors (14) were reported to be labeled *in vitro* with radiolabeled antagonists than with agonists, probably reflecting a difference in the receptor interaction with the G proteins (14). Similar conclusions can be drawn for sst$_2$ and sst$_3$ receptors labeled with antagonists, as shown in our Scatchard data. It appears, therefore, that, in an *in vivo* situation, an agonist that triggers a strong internalization but binds to a limited number of high-affinity receptors is a less-efficient targeting agent than an antagonist lacking internalization capabilities but binding to a larger variety of receptor conformations.

The long-lasting *in vivo* labeling of antagonists, in particular ^{111}In-DOTA-sst$_3$-ODN-8, may be brought in association to earlier findings by Wynn *et al.* (13) with gonadotropin-releasing hormone (GnRH) analogs. Although *in vitro* quantitative autoradiography did not detect any significant internalization at the electron-microscopic level of a GnRH antagonist during *in vitro* incubation for up to 120 min, *in vivo* cellular accumulation and binding of this antagonist to the pituitary GnRH receptor increased slowly during the 10 h after i.v. injection (13). These data were interpreted as reflecting the slow dissociation of the bound antagonist, with a persistence of specific binding up to 8 days after injection (13) but possibly also a delayed and slow internalization of the antagonist occurring 4–36 h after injection (13). Not to be ignored in this regard is that antagonists are also more chemically stable and more hydrophobic than agonists, resulting in longer duration of action and possible stabilization in the lipid-rich environment of the receptors.

What are the consequences of the present data for *in vivo* targeting of human cancers? First, after safety and efficacy evaluation in humans, radiolabeled DOTA-sst$_3$-ODN-8 should be evaluated in patients with sst$_3$-expressing tumors, such as inactive pituitary adenomas or pheochromocytomas (24, 25). Radiolabeled DOTA-sst$_2$-ANT should be studied in patients with sst$_2$-expressing tumors, consisting of a majority of neuroendocrine tumors. Then, it will be necessary to know whether the proposed change of paradigm can be generalized to other peptide receptor systems that are currently involved in peptide receptor targeting, including cholecystokinin, gastrin-releasing peptide, vasoactive intestinal peptide, neurotensin, and neuropeptide Y receptors (1). The answer to this question represents a long-term project for the nuclear oncology/molecular imaging community, requiring adequate tumor models, *in vitro* testing methods, and most importantly, adequate and potent antagonists as radioligands for the respective receptors. For the moment, peptidic antagonists are not available for every peptide receptor of interest and therefore need to be developed. The present results with ^{111}In-DOTA-sst$_3$-ODN-8 and ^{111}In-DOTA-sst$_2$-ANT, two radiolabeled peptide antagonists ready for nuclear medicine investigations, indicate the importance of developing such antagonist peptides. If the present observation can be confirmed for other receptors, the use of potent radiolabeled antagonists for *in vivo* tumor targeting may considerably improve the sensitivity of diagnostic procedures and the efficacy of receptor-mediated radiotherapy.

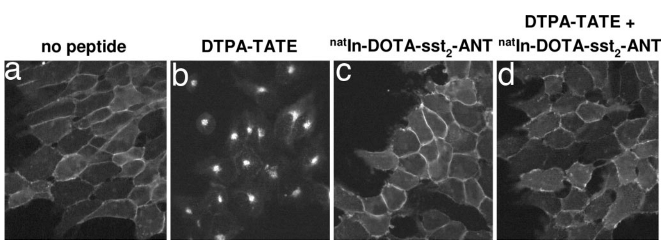

Fig. 3. Effect of somatostatin analogs on sst$_2$ internalization detected by immunofluorescence with R2–88 in HEK-sst$_2$ cells. Compared with control with no peptide (*a*), 100 nM DTPA-TATE (*b*) triggers strong sst$_2$ internalization. ^{nat}In-DOTA-sst$_2$-ANT (10 μM) (*c*) does not induce sst$_2$ internalization but abolishes internalization induced by 100 nM DTPA-TATE (*d*).

Materials and Methods

Peptides. Peptides were synthesized as described (18, 19). Radioactive or nonradioactive metals were chelated to the DOTA-coupled sst$_3$-ODN-8, DOTA-NOC, DOTA-sst$_2$-ANT, and DTPA-TATE, as described (21). The structure of DOTA-sst$_3$-ODN-8 is shown in Fig. 1*A*.

Cell Culture. The HEK293 cell lines (HEK-sst$_2$, HEK-sst$_3$) and the CCL39 cell lines (CCL-sst$_2$, CCL- sst$_3$) stably expressing the human sst$_2$ or sst$_3$ were grown as described (3, 26).

sst$_1$, sst$_2$, sst$_3$, sst$_4$, and sst$_5$ Receptor Binding *in Vitro*. The sst$_1$-, sst$_2$-, sst$_3$-, sst$_4$-, and sst$_5$-binding affinities of various compounds listed in Table 1 were measured by using *in vitro* receptor autoradiography, as described (26).

Saturation-binding experiments for $^{111/nat}$In-DOTA-sst$_2$-ANT and $^{111/nat}$DTPA-TATE or $^{111/nat}$In-DOTA-sst$_3$-ODN-8 and $^{111/nat}$In-DOTA-NOC were performed on HEK-sst$_2$ or -sst$_3$ cells, respectively, at 4°C by using increasing concentrations of the $^{111/nat}$In-labeled peptide ranging from 0.1 to 1,000 nM, as described (27). One micromolar cold peptide was used to quantify nonspecific binding. B_{max} was calculated for each radioligand from Scatchard plotting of the obtained data by using Origin 5.0 software (Microcal Software, Northampton, MA).

Adenylate Cyclase Activity. Forskolin-stimulated cAMP accumulation was determined in CCL-sst$_2$ and -sst$_3$ cells by using a commercially available cAMP scintillation proximity assay, as described (18).

sst$_2$ and sst$_3$ Receptor Internalization. Immunofluorescence microscopy-based internalization assay for sst$_2$ and sst$_3$ was performed as described (3). For sst$_3$ immunocytochemistry, the commercially available sst$_3$-specific antibody SS-850 (Gramsch Labora-

Table 4. Biodistribution in HEK-sst$_2$ tumor bearing nude mice after injection of ^{111}In-DOTA-sst$_2$-ANT or ^{111}In-DTPA-TATE

	^{111}In-DOTA-sst$_2$-ANT				^{111}In-DTPA-TATE		
Organ	0.5 h	4 h	4 h, blocked*	24 h	0.5 h	4 h	24 h
Blood	2.76 ± 0.19	0.14 ± 0.03	0.13 ± 0.01	0.05 ± 0.01	0.99 ± 0.25	0.13 ± 0.1	0.06 ± 0.01
Stomach	7.82 ± 2.03	0.61 ± 0.18	0.19 ± 0.07	0.25 ± 0.06	13.93 ± 8.16	7.04 ± 2.02	4.86 ± 1.68
Kidney	22.92 ± 2.62	10.5 ± 1.0	9.67 ± 1.38	7.38 ± 0.09	29.25 ± 7.7	11.44 ± 0.86	7.08 ± 1.21
Bowel	1.72 ± 0.25	0.16 ± 0.03	0.15 ± 0.03	0.08 ± 0.03	1.7 ± 0.53	0.97 ± 0.31	0.62 ± 0.16
Pancreas	24.16 ± 6.58	0.71 ± 0.21	0.09 ± 0.02	0.13 ± 0.02	18.18 ± 12.59	6.06 ± 3.26	2.26 ± 0.09
Spleen	1.67 ± 0.23	0.23 ± 0.04	0.21 ± 0.02	0.15 ± 0.02	1.13 ± 0.32	0.39 ± 0.05	0.21 ± 0.05
Liver	1.74 ± 0.18	0.43 ± 0.07	0.49 ± 0.03	0.32 ± 0.02	0.46 ± 0.07	0.16 ± 0.04	0.17 ± 0.03
Heart	1.23 ± 0.05	0.11 ± 0.03	0.08 ± 0.01	0.04 ± 0.0	0.53 ± 0.21	0.18 ± 0.07	0.1 ± 0.01
sst$_2$ tumor	**22.33 ± 3.27**	**29.12 ± 3.9**	**3.62 ± 0.26**	**22.84 ± 0.4**	**18.36 ± 4.37**	**15.83 ± 3.94**	**12.3 ± 1.32**
Muscle	0.97 ± 0.36	0.11 ± 0.02	0.09 ± 0.02	0.06 ± 0.03	0.51 ± 0.15	0.09 ± 0.03	0.05 ± 0.01
Adrenal	4.74 ± 3.0	0.49 ± 0.12	0.24 ± 0.04	0.46 ± 0.26	4.68 ± 1.46	1.95 ± 0.26	2.28 ± 0.67
Bone	1.84 ± 0.38	1.29 ± 0.75	0.58 ± 0.22	0.48 ± 0.14	0.8 ± 0.27	0.87 ± 0.65	0.74 ± 0.37
Pituitary	27.7 ± 6.48	20.23 ± 6.38	3.14 ± 0.91	2.08 ± 1.72	21.99 ± 5.36	12.1 ± 5.01	6.99 ± 4.61

The results are expressed in percent of the %IA/g, mean ± SEM, $n \geq 3$. Bold text indicates the tumor as the most important of the listed tissues.
*Blocked with excess DOTA-sst$_2$-ANT coinjected with the radioligand.

tories, Schwabenhausen, Germany) was used (3). For sst$_2$ immunocytochemistry, the sst$_2$-specific antibody SS-800 (Gramsch Laboratories) or the R2–88 antibody (A. Schonbrunn, Universtiy of Texas Health Science Center, Houston, TX) were used, with equivalent results, as reported (3, 28). HEK-sst$_2$ and -sst$_3$ cells were treated with the sst$_2$ or sst$_3$ agonists, respectively, at a concentration of 100 nM, or with agonists at a concentration of 100 nM in the presence of an excess of antagonists (100 times the concentration of the agonist) or with antagonists alone at a concentration of 10 μM and processed for immunofluorescence microscopy (3).

HEK-sst$_2$ and -sst$_3$ Cell Implantation in Nude Mice. Animals were kept, treated, and cared for in compliance with the guidelines of the Swiss regulations (approval 789). Athymic female nude mice were implanted s.c. with 10–12 million HEK-sst$_2$ and -sst$_3$ cells, respectively, freshly suspended in sterile PBS. Ten to fourteen days after inoculation, the mice showed solid palpable tumor masses (tumor weights, 60–150 mg) and were used for the *in vivo* biodistribution experiments.

Confirmation that the transfected tumors were indeed expressing solely sst$_2$ or sst$_3$, respectively, was obtained in resected tumor samples tested *in vitro* with somatostatin receptor autoradiography by using subtype selective ligands (24).

***In Vivo* Biodistribution of ^{111}In-Labeled Antagonists and Agonists.** Mice were injected into a tail vein with 10 pmol ^{111}In-radiolabeled peptide ($\approx$0.15–0.2 MBq) in 0.1 ml of NaCl solution (0.9%, with 0.1% BSA). To determine the nonspecific uptake of the radiolabeled peptides, mice were injected with 49 nmol sst$_3$-ODN-8 or ^{nat}In-DOTA-NOC (sst$_3$ study) or 20 nmol DOTA-sst$_2$-ANT (sst$_2$ study) in 0.05 ml of NaCl solution (0.9%) as a coinjection with the radioligand.

To study the biodistribution of ^{111}In-DOTA-sst$_3$-ODN-8, mice were killed at 0.25 h, 0.5 h, 1 h, 4 h, 24 h, or 72 h postinjection. For the biodistribution study of ^{111}In-DOTA-NOC or ^{111}In-DOTA-sst$_2$-ANT, mice were killed at 0.5 h, 4 h, or 24 h postinjection. The biodistribution of ^{111}In-DTPA-TATE was studied at 0.5 h or 4 h after injection. The organs of interest were collected, blotted dried, and weighed; their radioactivity was measured, and the %IA/g was calculated.

We thank V. Eltschinger, R. Kaiser, W. Low, and C. Miller for technical assistance and D. Doan and M. Kuonen for manuscript preparation. This work was supported by National Institutes of Health Grant R01 DK59953, National Science Foundation Grant 3100A0-100390, and the European Molecular Imaging Laboratories.

1. Reubi JC (2003) *Endocr Rev* 24:389–427.
2. Koenig JA, Edwardson JM (1997) *Trends Pharmacol Sci* 18:276–287.
3. Cescato R, Schulz S, Waser B, Eltschinger V, Rivier J, Wester HJ, Culler M, Ginj M, Liu Q, Schonbrunn A, *et al.* (2006) *J Nucl Med* 47:502–511.
4. Bodei L, Paganelli G, Mariani G (2006) *J Nucl Med* 47:375–377.
5. Hofland LJ, Lamberts SW (2003) *Endocr Rev* 24:28–47.
6. Weckbecker G, Lewis I, Albert R, Schmid HA, Hoyer D, Bruns C (2003) *Nat Rev Drug Discov* 2:999–1017.
7. Storch D, Behe M, Walter MA, Chen J, Powell P, Mikolajczak R, Macke HR (2005) *J Nucl Med* 46:1561–1569.
8. Gray JA, Roth BL (2001) *Brain Res Bull* 56:441–451.
9. Roettger BF, Ghanekar D, Rao R, Toledo C, Yingling J, Pinon D, Miller LJ (1997) *Mol Pharmacol* 51:357–362.
10. Bhowmick N, Narayan P, Puett D (1998) *Endocrinology* 139:3185–3192.
11. Pheng LH, Dumont Y, Fournier A, Chabot JG, Beaudet A, Quirion R (2003) *Br J Pharmacol* 139:695–704.
12. Liu Q, Cescato R, Dewi DA, Rivier J, Reubi JC, Schonbrunn A (2005) *Mol Pharmacol* 68:90–101.
13. Wynn PC, Suarez-Quian CA, Childs GV, Catt KJ (1986) *Endocrinology* 119:1852–1863.
14. Perrin MH, Sutton SW, Cervini LA, Rivier JE, Vale WW (1999) *J Pharmacol Exp Ther* 288:729–734.
15. Sleight AJ, Stam NJ, Mutel V, Vanderheyden PM (1996) *Biochem Pharmacol* 51:71–76.
16. Heppeler A, Froidevaux S, Eberle AN, Maecke HR (2000) *Curr Med Chem* 7:971–994.
17. Patel Y (1999) *Front Neuroendocrinol* 20:157–198.
18. Reubi JC, Schaer JC, Wenger S, Hoeger C, Erchegyi J, Waser B, Rivier J (2000) *Proc Natl Acad Sci USA* 97:13973–13978.
19. Wild D, Schmitt JS, Ginj M, Macke HR, Bernard BF, Krenning E, De Jong M, Wenger S, Reubi JC (2003) *Eur J Nucl Med Mol Imaging* 30:1338–1347.
20. Wild D, Macke HR, Waser B, Reubi JC, Ginj M, Rasch H, Muller-Brand J, Hofmann M (2005) *Eur J Nucl Med Mol Imaging* 32:724–724.
21. Ginj M, Chen J, Walter MA, Eltschinger V, Reubi JC, Maecke HR (2005) *Clin Cancer Res* 11:1136–1145.
22. de Jong M, Breeman WAP, Bakker WH, Kooij PPM, Bernard BF, Hofland LJ, Visser TJ, Srinivasan A, Schmidt MA, Erion JL, *et al.* (1998) *Cancer Res* 58:437–441.
23. Bass RT, Buckwalter BL, Patel BP, Pausch MH, Price LA, Strnad J, Hadcock JR (1996) *Mol Pharmacol* 50:709–715.
24. Reubi JC, Waser B, Schaer JC, Laissue JA (2001) *Eur J Nucl Med* 28:836–846.
25. Mundschenk J, Unger N, Schulz S, Hollt V, Steinke R, Lehnert H (2003) *J Clin Endocrinol Metab* 88:5150–5157.
26. Reubi JC, Schaer JC, Waser B, Wenger S, Heppeler A, Schmitt J, Mäcke HR (2000) *Eur J Nucl Med* 27:273–282.
27. Ginj M, Hinni K, Tschumi S, Schulz S, Maecke HR (2005) *J Nucl Med* 46:2097–2103.
28. Korner M, Eltschinger V, Waser B, Schonbrunn A, Reubi JC (2005) *Am J Surg Pathol* 29:1642–1651.